Pure appl. geophys. 161 (2004) 2125–2137
0033–4553/04/122125–13
DOI 10.1007/s00024-004-2553-y

Pure and Applied Geophysics

Guided Waves from Sources Outside Faults: An Indication for Shallow Fault Zone Structure?

MIKO FOHRMANN[1,3], HEINER IGEL[1], GUNNAR JAHNKE [1,4], and YEHUDA BEN-ZION [2]

Abstract — Using 3-D numerical modeling of seismic wave propagation we investigate the possibility of generating fault zone (FZ) trapped wave energy from sources well outside a fault. The FZ is represented by a O(200 m) wide vertical low velocity layer in a half space. We find that FZ trapped waves can be excited from sources well outside the fault if (1) the low-velocity structure extemds only to shallow depth and the source is located at greater depth or (2) the structure of the low-velocity zone is such that only the shallow part of the FZ traps energy. FZ trapped waves are not excited from sources well outside a FZ continuous with depth. The results support, in conjunction with recent observational evidence, a model for natural faults with shallow trapping structures rather than ones that span the entire seismogenic zone. This may have implications for fault mechanics as well as for aspects of shaking hazard near faults.

Key words: Wave propagation, fault zones, trapped waves, seismic hazard.

Introduction

In the last two decades fault zone (FZ) trapped waves have been observed along several earthquake faults with receivers close to the FZ (e.g., CORMIER and SPUDICH, 1984; LI and LEARY, 1990; HOUGH *et al.*, 1994). There have been claims that analysis of such phases may be used to provide a higher resolution imaging of FZ structure at seismogenic depth than is possible with standard ray-tomographic methods.

Several theoretical studies were carried out in order to investigate the trapping efficiency in simple and somewhat complex fault geometries. The 2-D analytical solution of Ben-Zion and Aki (1990) was used extensively to explore the influence of various FZ parameters (e.g., BEN-ZION, 1998) and to model observations (e.g., MICHAEL and BEN-ZION, 1998; BEN-ZION *et al.*, 2003). LEARY *et al.* (1991),

[1] Department Earth and Environmental Sciences, Ludwig-Maximilians-University, Theresienstrasse 31, 80333 Munich, Germany. E-mail: Heiner.Igel@lmu.de.

[2] Department of Earth Sciences, University of Southern California, Los Angeles, CA 90089-0740, U.S.A.

[3] Now at: Geology Department, University of Otago, Leith Street, PO Box 56, Dunedin, New Zealand. E-mail: fohmi830@student.otago.ac.nz

[4] Now at: Bundesanstalt für Geowissenschaften und Rohstoffe, Stilleweg 2, 30655 Hannover

HUANG *et al.* (1995), LI and VIDALE (1996), IGEL *et al.* (1997, 2002), JAHNKE *et al.* (2002), and others performed numerical simulations of 2-D and 3-D fault geometries with the goal of investigating the influence of non-uniform FZ structures on the wavefield observed at the surface.

In recent studies, IGEL *et al.* (2002) and JAHNKE *et al.* (2002) attempted to classify important (e.g., structural discontinuities) and less important (e.g., vertical velocity gradients, small geometrical deviations from planar faults) effects on the trapping efficiency due to non-planar structures. In most previous theoretical studies the source location was chosen to be either within or at the boundary of the FZ, in line with arguments of observational studies (e.g., Li *et al.*, 1994, 2000) suggesting that FZ guided waves are only generated when the sources are close to or inside the low-velocity FZ layer. Based on these works, it was thought that only a small percentage of earthquakes in an active fault generate FZ trapped waves. Recently, observations above the Karadere-Duzce branch of the North Anatolian fault have shown that trapped wave energy is generated by earthquakes occurring in a large volume around the active fault (BEN-ZION *et al.*, 2003). As illustrated in the following sections, this indicates that the trapping structure is shallow rather than extending throughout the seismogenic crust. Shallow trapping structures were also inferred in other studies of active and inactive faults by HABERLAND *et al.* (2001), ROVELLI *et al.* (2002), and PENG *et al.* (2003) and KORNEEV *et al.* (2003).

In this study we discuss numerical simulations of 3-D wave propagation which show that sources at considerable distance from the FZ are able to generate high amplitude trapped waves. We focus on a structure consisting of a shallow low velocity FZ layer (depth < 5 km) in a half space, and perform a parameter study quantifying the amplification of ground motion for sources outside and below the FZ layer. In general, the trapping efficiency depends on the source mechanism and orientation of the source with respect to the FZ layer. We employ strike-slip sources and examine fault-parallel particle motion. Similar conclusions are expected for other source types and corresponding particle motion.

The generation of guided waves by sources well outside the FZ has implications for shaking hazard close to faults (SPUDICH and OLSEN, 2001). It further highlights the need for considerable care and support from additional evidence when interpreting fault zone trapped waves in terms of low velocity zones that extend throughout the seismogenic crust.

Trapped Waves from Sources Outside Fault Zones

To investigate the trapping efficiency of various fault zone models and source positions we carry out 3-D numerical calculations using a finite-difference method. The algorithm was carefully checked against analytical solutions (BEN-ZION, 1990; BEN-ZION and AKI, 1990) for sources at or close to material boundaries (IGEL *et al.*,

Table 1

Parameters for 3-D fault simulations. The FZ velocities and the density are lowered by 30% with respect to the surrounding half space.

Grid size	$400 \times 700 \times 400$
Model size	11km × 20 km × 12 km
Source type	$M_{xy} = M_{yx} = M_0$
Dominant frequency	8 Hz
Grid spacing	30 m
Time step	1.7 ms
Fault zone width	180 m
Receiver spacing	30 m

	P-wave-velocity [m/s]	*S*-wave-velocity [m/s]	Density [kg/m^3]
Host Rock	5000	3100	2350
Fault Zone	3500	2170	1645

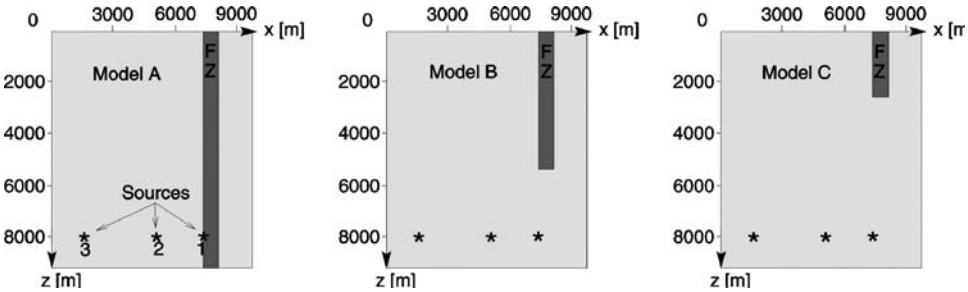

Figure 1

Fault models and source positions of the 3-D simulations. Receivers are positioned on profiles across the fault in the vertical plane through the source positions and displaced in the *y*-direction.

2002). The parameters of the simulations are summarized in Table 1. The model geometry is illustrated in Figure 1. Three different fault zone models are used: A: deep FZ continuous with depth; B: FZ extending to intermediate depth; C: shallow FZ. Sources 1–3 are positioned below the fault or with some offset in the horizontal direction.

The source has a strike-slip dislocation mechanism with $M_{xy} = M_{yx} = M_0$ being the only non-zero moment tensor components. The geometry of the receiver array is illustrated in Figure 2. The receiver sampling right above the fault is 30 m. In vertical planes through the source locations perpendicular to the fault (and small to moderate angels to such planes) predominantly fault-parallel motion (*y*-component, SH-type) is generated. Therefore, only *y*-component synthetic seismograms are shown.

We first consider the situation in which the source is outside a FZ continuous with depth. Although it is known that such a geometry will not produce trapped wave energy (e.g., BEN-ZION, 1998; JAHNKE *et al.*, 2002), we use this model as a reference.

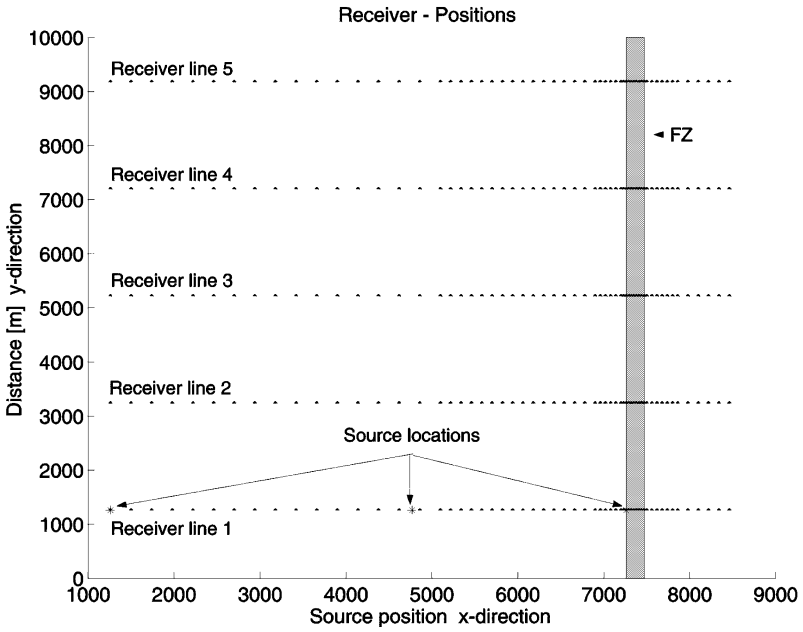

Figure 2
Position of the receiver strings at the free surface with respect to fault zone and epicenters. Above the fault the receiver spacing is 30 m. The symmetry with respect to the fault zone is exploited when evaluating source volumes which are capable of producing trapped wave energy.

y-component seismograms for source position 2 (Fig. 1, model A) are shown in Figure 3. The direct *S* wave is the signal with the largest amplitude above the fault. The direct wave is reflected by the fault boundary. No trapping of seismic energy is visible.

The situation is different when the depth range of the FZ is shallower than the source depth. Snapshots of *y*-component motion for a shallow fault (model C) and source position 2 outside the fault (see Fig. 1) at two time steps are shown in Figure 4. Considerable energy enters the fault from below, resulting in high amplitude trapped waves observable at the surface. To address the issue of whether the shape of the lower FZ end influences the trapping efficiency, we performed additional simulations with pencil-shaped low-velocity structures of varying angles. Figure 5 gives seismograms for the shallow FZ with flat bottom and the two pencil-shaped FZs (Fig. 5, top right). The seismograms of the three different models are very similar. We conclude that the particular geometry of the fault zone end has negligible effects on the trapping efficiency.

In Figure 6 the *y*-component seismograms for the model setup of Figure 4 are shown. In addition to the direct *S* wave there are signals with maximum amplitudes larger than the direct *S* wave for receivers above the fault. The amplitudes of these signals rapidly decay with distance from the fault, indicative of FZ trapped waves.

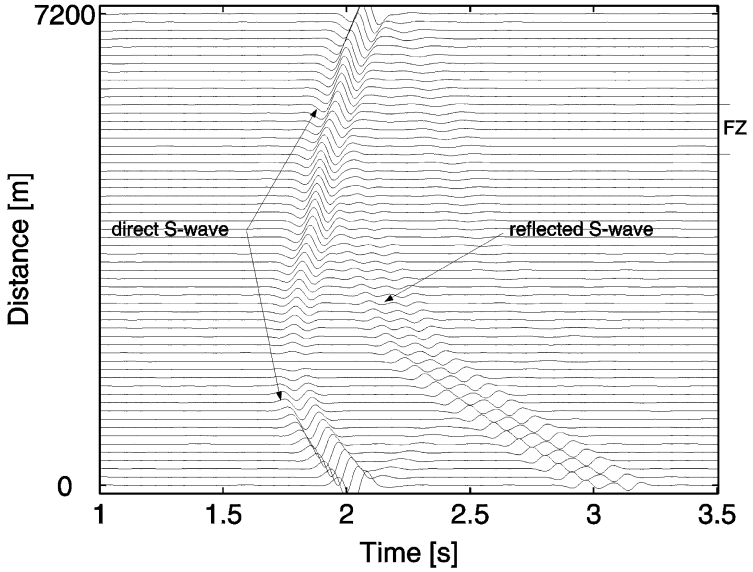

Figure 3
Synthetic seismograms (y-component of horizontal velocity) of model A recorded on receiver line 1 for source position 2 outside the FZ. The region above the fault is denoted by "FZ". No trapped wave energy is visible. The direct S wave and the reflections from the FZ can be identified.

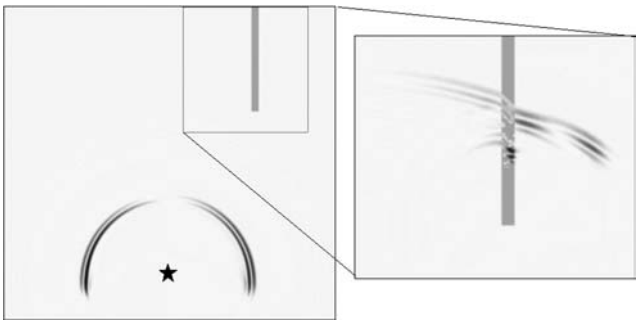

Figure 4
Snapshots at two different times for shallow fault model C and source position 2 (star). The shallow fault zone is capable of trapping energy even for a source position well outside it.

To quantify these observations for a large number of source positions we examine the source volume that can lead to trapped waves in a shallow fault zone structure. Using time windows containing either the direct S wave or the trapped waves, we calculate the ratio of trapped wave to S-wave energy recorded at a particular receiver at the surface on the fault. This is done for numerous source positions and source-receiver paths. Examples of time windows used to calculate the energy ratios are shown in Figure 7. To reduce the number of numerical simulations we exploit the

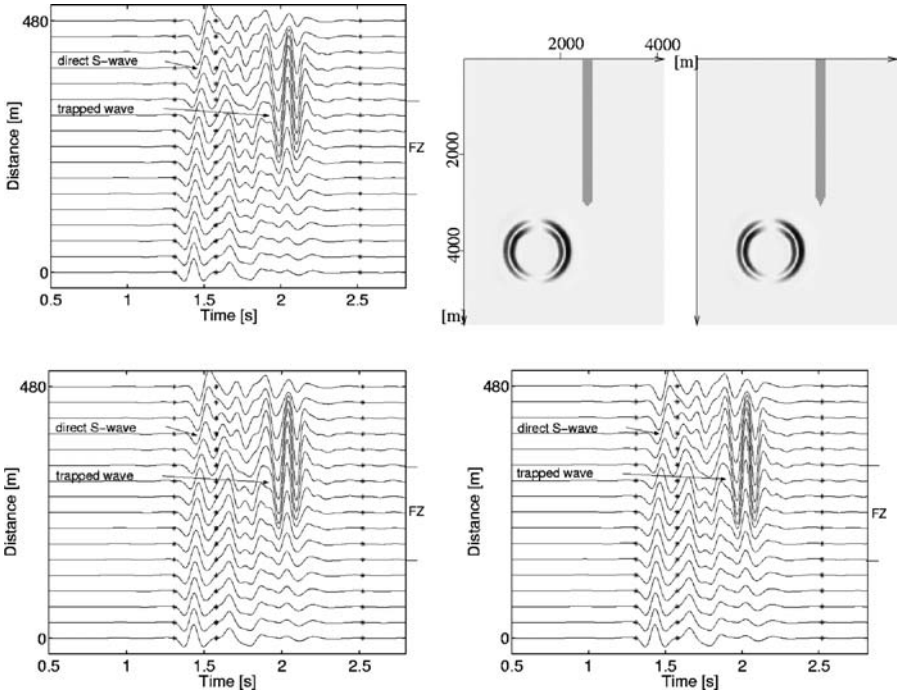

Figure 5
Top left: Synthetic seismograms (y-component of horizontal velocity) for a shallow FZ model with flat bottom end. Top right: Geometry of pencil shaped FZ ends. Bottom left and right: Synthetic seismograms (y-component of horizontal velocity) for the left and right shapes, respectively.

symmetry of the problem and pose numerous receiver lines offset in the y-direction (Fig. 2).

Using the above procedure we compute the energy ratio for a large number of source-receiver paths with respect to the FZ for fault model B (intermediate depth, see Fig. 1). The geometry of the model setup is illustrated with more detail in Figure 8 (top left). The ratio of trapped wave to direct S-wave energy is calculated for a receiver placed at the surface and at the center of the fault for all source positions. This enables us to allocate to each source position at depth the corresponding energy ratio it produces at our receiver at the surface.

To visualize the results of this regular 3-D grid of energy ratios at depth we calculate (through interpolation) iso-surfaces which contain sources that lead to ratios exceeding a particular value. Such surfaces are shown in Figure 8 (top right and bottom) for several ratios (2, 5, and 10). Significantly, the results show that five- and ten-fold amplifications with respect to the direct S wave are produced for sources several kilometers away from the fault (Fig. 8, bottom right). Note that the volumes are open to greater depths, indicating that such amplifications are possible for sources with a greater depth range than was covered by our numerical simulations.

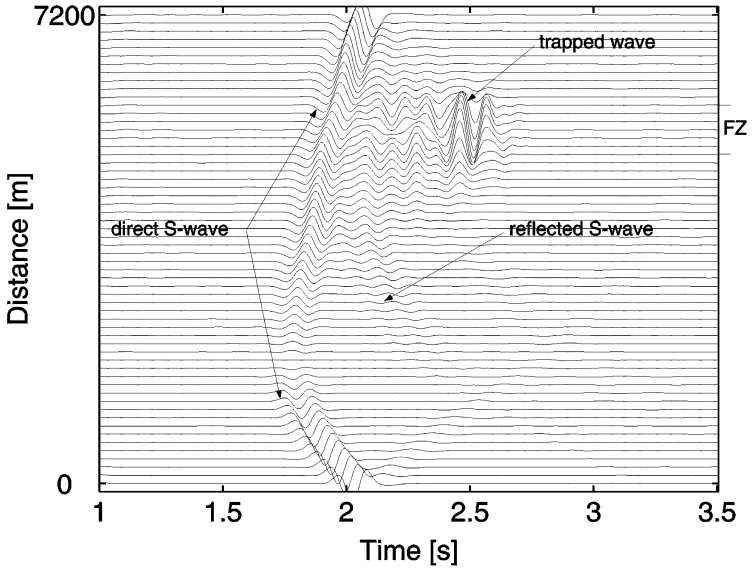

Figure 6
Synthetic seismograms (y-component of horizontal velocity) of model C recorded on receiver line 1 for source position 2 outside the FZ.

The size and shape of such volumes strongly depend on the source type (orientation of fault plane, and slip direction), the FZ properties (e.g., velocity contrast, depth extent), and wavelength of the wavefield with respect to the FZ width. With a mixture of focal mechanisms expected to exist in aftershock sequences on active faults, the volume of sources generating trapped waves in the shallow FZ structure can be considerably larger than that shown in Figure 8. Indeed, BEN-ZION *et al.* (2003) found that trapped waves are generated on the Karadere-Duzce branch of the North Anafolian fault by aftershocks of the 1999 Izmit earthquake located in a large volume around the Karadere–Duzce fault.

If trapped wave energy can be generated in shallow structures, does this imply that there are no low-velocity FZ layers at greater depth? To answer this question we simulate two further depth-dependent FZ structures (Fig. 9). First, a source is located outside a FZ which is offset (by one FZ width) in the direction away from the source at greater depth. The seismograms show that—while a continuous FZ would not trap energy—the shallow part of the discontinuous structure does lead to high-amplitude trapped waves. The FZ structure below the discontinuity has no influence on the trapped waves by this source-receiver geometry.

The same conclusions hold for a structural disruption consisting of a bottleneck at the same depth as the previous discontinuity (Fig 9, bottom). The trapping efficiency is similar to the previous case and the trapping occurs again only in the shallow part above the bottleneck structure. These results indicate that FZ trapped

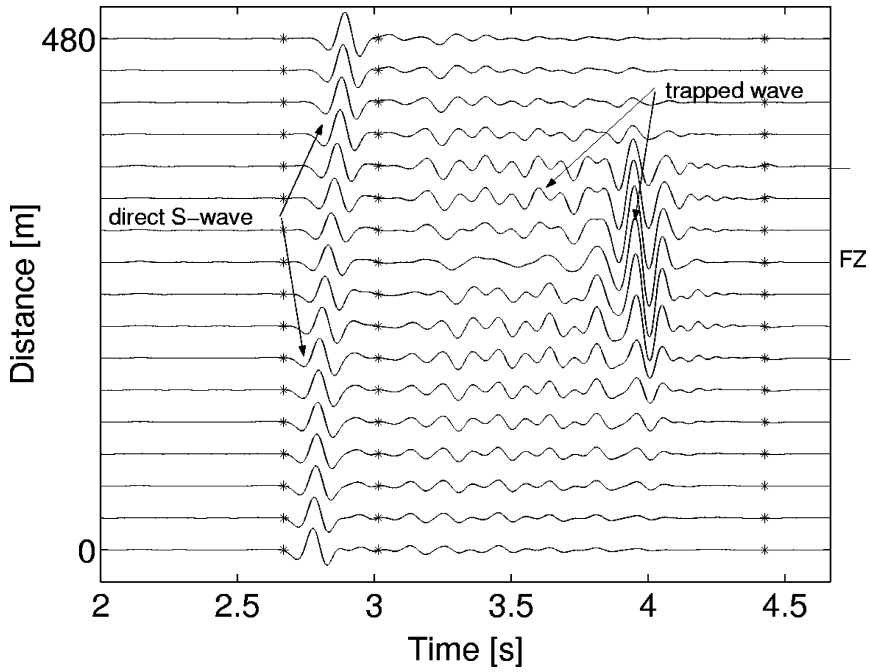

Figure 7
Synthetic seismograms (y-component of horizontal velocity) of model B recorded on receiver line 1 close to the fault for source position 2 outside the FZ. The stars mark time windows which are used to calculate the ratio of energy between S wave and trapped wave phases.

waves generated by sources outside the FZ, and therefore indicative of shallow structures, do not exclude the possibility of deeper low-velocity FZ layers. However, these deeper structures are not illuminated by the trapped waves, as those are generated only by the shallower sections above the severe structural disruptions.

FZ trapped waves are associated with particle motion parallel to the FZ walls. Several types of sources can produce such motion *purely*. These include strike-slip faulting, dip-slip faulting and detachment along a horizontal plane, all with proper orientation with respect to the fault. Other source mechanisms can have a component that produces particle motion parallel to the fault. We note that the data set of BEN-ZION *et al.* (2003) recorded on the Karadere-Duzce branch of the North Anatolian fault probably includes several or all of these types of sources. The results so far focused only on pure SH motion generated by strike-slip sources. Such sources produce considerable trapped waves energy when the events are located at some distance from the fault, since the fault is a nodal plane for radiation from a strike-slip source. The radiation pattern in the plane through source and receiver (see Fig. 5, top right, and Figure 10, red line) explains the gap

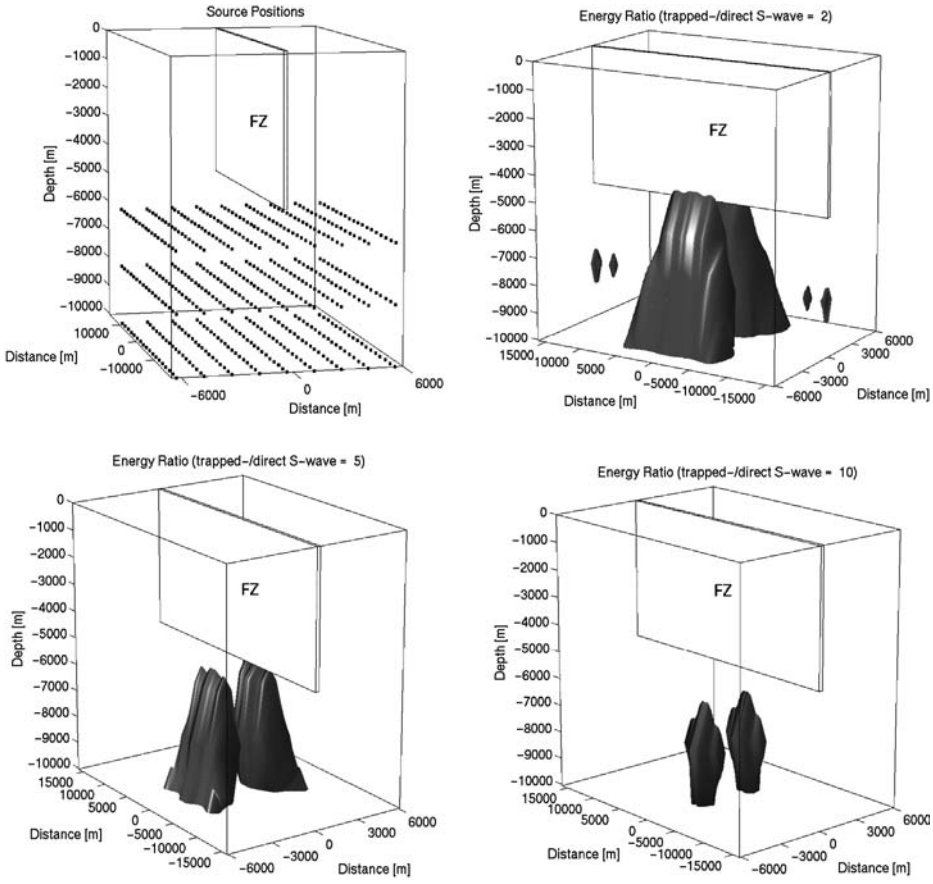

Figure 8
Top left: Source positions (only every 15th in y-direction is shown) used to estimate the volume which is capable of producing trapped wave energy exceeding the S-wave energy. Top right: Volume in which the energy ratio between trapped waves and S waves exceeds a factor 2. Bottom left: Volume for a ratio of 5. Bottom right: Volume for ratio of 10.

between the iso-surfaces for a given amplification of FZ trapped waves (Fig 8). However, other source mechanisms will have different iso-surfaces for motion amplification in the FZ that will augment the results of Figure 8. For example, the radiation pattern for SV-type motion generated by dip-slip events (Fig. 10, solid line) is complementary to that associated with SH motion generated by strike-slip events (Fig. 10, dashed line). It is thus clear that the volume of sources capable of generating motion amplification inside the FZ in a complex tectonic domain, with a variety of source mechanisms, can be considerably larger than that shown in Figure 8.

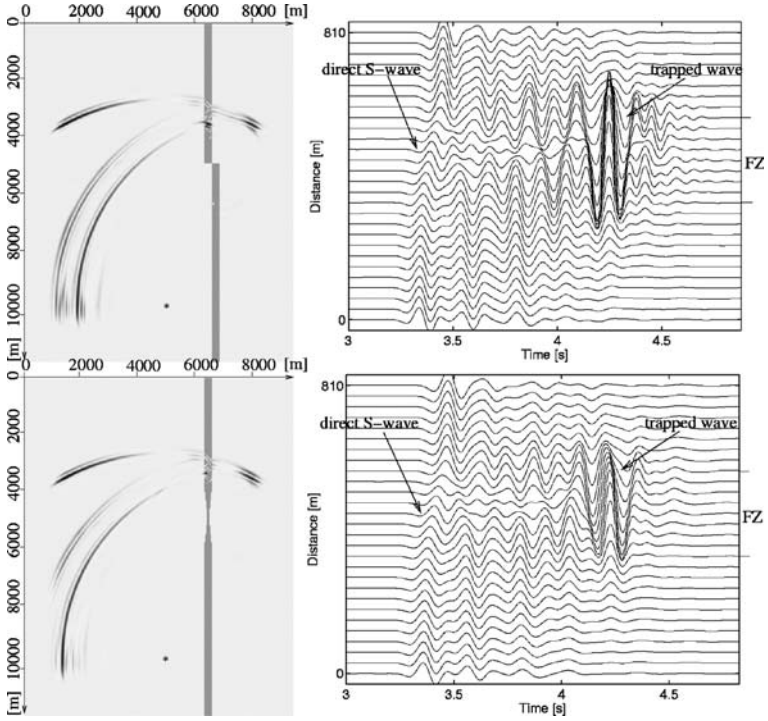

Figure 9
Top left: Snapshot for offset fault model and source position 2 (star). Only the shallow fault zone (upper part) is capable of trapping energy for a source position well outside it. Top right: Synthetic seismograms (y-component of horizontal velocity) for discontinuous FZ model. Bottom left: Snapshot for bottleneck fault model and source position 2 (star). Bottom right: Synthetic seismograms (*y*-component of horizontal velocity) for bottleneck model. The energy enters the FZ only at the bottleneck.

Discussion and Conclusions

The velocity structure of FZs at depth and near the surface has important implications for the dynamic behavior of faults as well as the expected ground motion for earthquake scenarios in those regions. As ray-based methods are not capable of resolving the small scales involved, other methods are needed to provide this information. FZ guided waves are now commonly observed with receivers positioned directly above the surface traces of fault zones. Over the past decade various studies suggested that the trapping structures extend to the bottom of the seismogenic zone.

There is now substantial evidence from observations (HABERLAND *et al.*, 2001; BEN-ZION *et al.*, 2003; ROVELLI *et al.*, 2002; PENG *et al.*, 2003) that the low-velocity zone associated with faults which is capable of trapping energy is likely to be a shallow feature. BEN-ZION *et al.* (2003) report that most aftershocks—originating

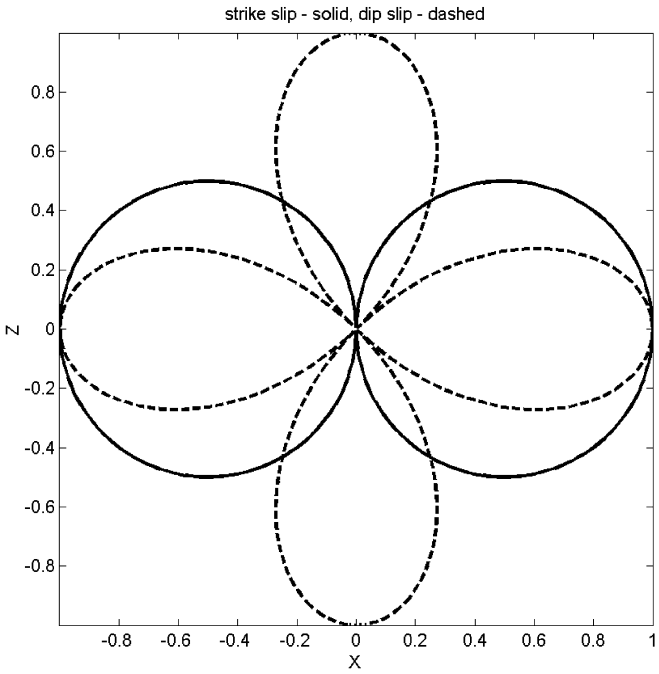

Figure 10
Radiation pattern of shear waves in a plane through the source and receiver. Solid: SH type motion for strike-slip source. Dashed: SV type motion for dip-slip source.

in a large crustal volume—recorded on or close to the North Anatolian fault generate considerable trapped wave motion. This indicates that a shallow (near vertical) low-velocity structure below the receivers on the fault is responsible for the observed trapped waves. While many of the trade-offs of FZ parameters for uniform FZ structures were previously discussed (e.g., BEN-ZION, 1998), the fact that FZs may be shallow features points to a further ambiguity when inverting trapped waveforms.

In this study we explored the possibility of generating FZ trapped waves from sources well outside shallow fault structures. The conclusions are that (1) considerable trapping efficiency is possible for sources well outside a shallow fault zone; (2) large source volumes are able to generate local amplification above faults; and (3) in the presence of discontinuous structures, trapped waves from the shallow part may obscure low-velocity structures at greater depth. The amplification from large source volumes at FZ stations was coined "fault zone related site effects" by BEN-ZION *et al.* (2003). The relevance of such amplifications to shaking hazard was previously pointed out by SPUDICH and OLSEN (2001).

The reliable estimation of fault zone structure at depth still poses a considerable challenge to both experimental and theoretical seismology.

Acknowledgements

The study was facilitated by a visit of YBZ to Munich supported by the German Academic Exchange Service through the IQN-Georisk (www.iqn-georisk.de) and through a Mercator Fellowship by the German Research Foundation. We thank the Leibniz Rechenzentrum Munich for access to their supercomputers. The work was partially supported through the KONWIHR network and also benefited from the BaCaTec initiative. YBZ acknowledges support from the National Science Foundation (grant EAR0003401).

References

Ben-Zion, Y. (1990), *The Response of Two Half Spaces to Point Dislocations at the Material Interface*, Geophys. J. Int. *101*, 507–528.

Ben-Zion, Y. (1998), *Properties of Seismic Fault Zone Waves and their Utility for Imaging Low-velocity Structures*, J. Geophy. Res. *103*, 12,567–12,585.

Ben-Zion, Y. and Aki, K. (1990), *Seismic Radiation from an SH Line Source in a Laterally Heterogeneous Planar Fault Zone*, Bull. Seismol. Soc. Am. *80*, 971–994.

Ben-Zion, Y., Peng, Z., Okaya, D., Seeber, L., Armbruster, J.G., Ozer, N., Michael, A. J., Baris, S., and Aktar, M. (2003), *A Shallow Fault Zone Structure Illuminated by Trapped Waves in the Karadere-Duzce Branch of the North Anatolian Fault, Western Turkey*, Geophys. J. Int. *152*, 699–717.

Cormier, V. F., and Spudich, P. (1984), *Amplification of Ground Motion and Waveform Complexities in Fault Zones: Examples from the San Andreas and Calaveras Faults*, G. J. Roy. Astr. Soc. *79*, 135–152.

Haberland, C., Maercklin, N., Ryberg, T., Rumpker, G., Weber, M., Agnon, A., El-Kelani, R., Qabbani, I., and Scherbaum, F. (2001), *Observation of Guided Waves at the Wadi Arava Fault, Jordan*, EOS Trans, Am. Geophys. Union *82*, F885.

Hough, S. E., Ben-Zion, Y., and Leary, P. C. (1994), *Fault-zone Waves Observed at the Southern Joshua Tree Earthquake Rupture zone*, Bull. Seismol. Soc. Am. *8*, 761–767.

Huang, B. S., Teng, T.-L., and Yeh, Y. T. (1995), *Numerical Modeling of Fault-zone Trapped Waves: Acoustic Case*, Bull. Seismol. Soc. Am. *85*, 1711–1717.

Igel, H., Ben-Zion, Y., and Leary, P. (1997), *Simulations of SH- and P-SV-wave Propagation in Fault Zones*, Geophys. J. Int. *128*, 533–546.

Igel, H., Jahnke, G., and Ben-Zion, Y. (2002), *Numerical Simulation of Fault Zone Guide Waves: Accuracy and 3-D Effects*, Pure Appl. Geophys. *159*, 2067–2083.

Jahnke, G., Igel, H., and Ben-Zion, Y. (2002), *Three-dimensional Calculations of Seismic Fault Zone Waves in various Irregular Structures*, Geophys. J. Int. *151*, 416–426.

Korneev, V.A., Nadeau, R.M. and McEvilly, T.V. (2003), *Seismological studies at Parkfield IX: Fault-zone imaging using guided wave attenuation*, Bull. Seism. Soc. Am., *93*, 1415–1426.

Leary, P. C., Igel, H., and Ben-Zion, Y. (1991) *Observation and modeling of fault zone trapped waves in aid of precise precursory microearthquake location and evaluation, Earthquake Prediction: State of the Art*, Proc. Internat. Conf., Strassbourg, France, 15–18 October 1991, pp. 321–328.

Li, Y. G., Aki, K., Adams, D., and Hasemi, A. (1994), *Seismic Guided Waves Trapped in the Fault Zone of Landers, California, Earthquake of 1992*, J. Geophys. Res., *99* (B6), 11,705–722.

Li, Y. G., and Vidale, J. E. (1996), *Low-velocity Fault-zone Guided Waves: Numerical Investigations of Trapping Efficiency*, Bull. Seismol. Soc. Am. *86*, 371–378.

Li, Y. G. Vidale, J. E., Aki, K., and Xu, F. (2000), *Depth-dependent Structure of the Landers Fault zone From Trapped Waves Generated by Aftershocks*, J. Geophys. Res. *105*, 6237–6254.

Li, Y. G. and Leary, P. C. (1990), Fault Zone Seismic Trapped Waves, Bull. Seismol. Soc. Am. *80*, 1245–1271.

MICHAEL, A. J. and BEN-ZION, Y. (1998), *Inverting Fault Zone Trapped Waves with a Genetic Algorithm*, EOS Trans. Am. Geophys. Union *79*, F584.

PENG, Z., BEN-ZION, Y., MICHAEL, A. J., and ZHU, L. (2003), *Quantitative Analysis of Seismic Trapped Waves in the Rupture Zone of the Landers, 1992, California Earthquake: Evidence for a shallow Trapping Structure*, Geophys. J. Int., *155*, 1021–1041

ROVELLI, A., CASERTA, A., MARRA, F., and RUGGIERO, V. (2002), *Can Seismic Waves be Trapped Inside an Inactive Fault Zone? The Case Study of Nocera Umbra, Central Italy*, Bull. Seismol. Soc. Am. *92*(6), 2217–2232.

SPUDICH, P. and OLSON, K.B. (2001), *Fault Zone Amplified Waves as a Possible Seismic Hazard along the Calaveras Fault in Central California*, Geophys. Res. Lett. *28*(13), 2533–2536.

(Received September 27, 2002, revised April 25, 2003, accepted May 5, 2003)